UDC 681.516 https://doi.org/10.20998/2074-272X.2026.1.06

Q.B. Nguyen, X.C. Nguyen

Finite-time robust position tracking control for DC motors under uncertain dynamics

Introduction. *This study proposes a finite-time robust control law for position tracking of a DC motor under conditions of model uncertainty and external disturbances. The motor operates through a pulse-width modulation (PWM) unit and an H-bridge power circuit, aiming to achieve finite-time position tracking while minimizing the effects of model uncertainties and external disturbances.* ***Problem.*** *The main challenge lies in achieving accurate and rapid position and speed regulation for the DC motor while maintaining high performance, despite model inaccuracies and external disturbances. The* ***goal*** *of this paper is to design a robust finite-time position tracking control law for a DC motor based on the differential geometric approach, ensuring high tracking accuracy and control efficiency in the presence of disturbances and parameter uncertainties.* ***Scientific novelty.*** *The integration of finite-time control based on a virtual system, diffeomorphism transformation, and disturbance compensation introduces an innovative solution for DC motor position tracking under incomplete modeling and external perturbations.* ***Methodology.*** *The study employs the differential geometric method to construct a virtual system with finite-time characteristics and uses Lyapunov theory to prove global stability in the presence of uncertainties and disturbances. A finite-time virtual system is proposed after analyzing the incomplete dynamic model of the DC motor.* ***Results.*** *To validate the proposed approach, MATLAB simulations were conducted and compared with a conventional sliding mode controller. The results demonstrate improved settling time and robustness of the proposed method in DC motor position tracking. The findings confirm that the proposed controller provides intuitive and precise control, accurate position tracking, and enhanced performance regulation. It also exhibits strong robustness against model uncertainties and external disturbances. The* ***practical value*** *of the proposed method is considerable, as it offers a reliable and efficient position control scheme for DC motors using PWM. The method ensures precise position control and robust performance under varying conditions and external interferences, making it well-suited for real-world DC motor control applications.* References 23, tables 1, figures 12.

Key words: **DC motor, finite-time control, sliding mode control, diffeomorphism transformation, differential geometric method.**

Вступ. *У дослідженні пропонується робастний закон керування зі скінченним часом для відстеження положення двигуна постійного струму в умовах невизначеності моделі та зовнішніх збурень. Двигун працює через блок широтно-імпульсної модуляції (PWM) та схему живлення Н-подібного моста, метою чого є досягнення відстеження положення зі скінченним часом, мінімізуючи вплив невизначеностей моделі та зовнішніх збурень.* ***Проблема***. *Основна проблема полягає в досягненні точного та швидкого регулювання положення та швидкості двигуна постійного струму, зберігаючи при цьому високу продуктивність, незважаючи на неточності моделі та зовнішні збурення.* ***Метою*** *роботи є розробка робастного закону керування відстеженням положення двигуна постійного струму зі скінченним часом на основі диференціально-геометричного підходу, що забезпечує високу точність відстеження та ефективність керування за наявності збурень та невизначеностей параметрів.* ***Наукова новизна***. *Інтеграція керування зі скінченним часом на основі віртуальної системи, перетворення дифеоморфізму та компенсації збурень пропонує інноваційне рішення для відстеження положення двигуна постійного струму за неповного моделювання та зовнішніх збурень.* ***Методологія***. *У дослідженні використовується диференціально-геометричний метод для побудови віртуальної системи з характеристиками зі скінченним часом та теорія Ляпунова для доведення глобальної стійкості за наявності невизначеностей та збурень. Після аналізу неповної динамічної моделі двигуна постійного струму запропоновано віртуальну систему зі скінченним часом.* ***Результати***. *Для перевірки запропонованого підходу було проведено моделювання в MATLAB та порівняно зі звичайним контролером ковзного режиму. Результати демонструють покращений час встановлення та стійкість запропонованого методу відстеження положення двигуна постійного струму. Отримані дані підтверджують, що запропонований контролер забезпечує інтуїтивно зрозуміле та точне керування, точне відстеження положення та покращене регулювання продуктивності. Він також демонструє високу стійкість до невизначеностей моделі та зовнішніх збурень.* ***Практична значимість*** *запропонованого методу є значною, оскільки він пропонує надійну та ефективну схему керування положенням для двигунів постійного струму з використанням PWM. Метод забезпечує точне керування положенням та стійку роботу за різних умов та зовнішніх перешкод, що робить його добре придатним для реальних застосувань керування двигунами постійного струму.* Бібл. 23, табл. 1, рис. 12.

Ключові слова: **двигун постійного струму, кінцеве керування, ковзний режим керування, дифеоморфне перетворення, диференціально-геометричний метод.**

Introduction. A DC motor has been widely applied in various fields such as robotics, servo systems, biomedical devices, and embedded systems due to its simple structure, ease of control, and low cost [1, 2]. However, achieving precise control of DC motors remains a significant challenge because of their strong nonlinear characteristics, parameter uncertainties (such as friction, inductance, and back electromotive force), and external disturbances including load variations or dead zones [3]. In particular, for small-scale DC motors driven by pulse-width modulation (PWM), direct measurement of the armature current is often difficult, which highlights the need for developing control strategies based on incomplete or uncertain models [4].

Over the past decades, numerous control approaches have been proposed to improve the trajectory-tracking performance of DC motors. However, the conventional PID control method cannot accurately capture the dynamic variations of motor excitation [4, 5]. Consequently, with the growing interest in nonlinear systems, a wide range of control theories and techniques related to nonlinear dynamics have been employed to address DC motor drive control problems, such as backstepping control [3], sliding mode control (SMC) [6, 7], adaptive control [8, 9], fuzzy control [2, 10], neural network-based control [11], and robust control [12]. In studies [13–15], several optimization-based methods were proposed for tuning controller parameters using nature-inspired optimization algorithms, aiming to minimize steady-state error and shorten the transient response. However, these studies did not consider the finite-time response of the system and were limited to ensuring only asymptotic stability.

The finite-time control technique [16–19] offers significant advantages, including rapid response,

predefined convergence time, and strong robustness against disturbances. The application of finite-time control in tracking problems has yielded remarkable results. In many practical cases, DC motors require real-time control, and the system must achieve stability within a short period. Therefore, employing finite-time control techniques for DC motors under disturbances and model uncertainties has attracted considerable attention from researchers seeking to enhance control performance. In [16], a controller was developed to ensure that the transient motion process is almost completed within a predetermined finite time, after which the desired trajectory is tracked with a specified precision. In [17], a novel finite-time disturbance observer was proposed for trajectory tracking of DC motors with model uncertainties and exogenous disturbances. The application of finite-time control has also produced impressive results in electromechanical systems with DC motor actuators, as reported in [18, 19]. Furthermore, studies [20–23] have introduced an approach to control law design based on the diffeomorphic control method. This method utilizes geometric transformations to map the actual system into a simplified virtual system, enabling the design of a control law that ensures the real system states are embedded into a desired invariant manifold [20]. The main advantage of diffeomorphic control lies in its flexible design framework, which can be readily extended to various nonlinear systems, allowing the designer to specify desired manifold properties directly.

Purpose and objectives of the article. This paper proposes a synthesis technique for a finite-time robust control law based on geometric control theory. The approach involves constructing a virtual system with both asymptotic and finite-time stability properties and establishing a diffeomorphic transformation between the real and virtual systems to derive the control law. The proposed control law ensures the equivalence of dynamic properties between the real and virtual systems, meaning that the real system also achieves finite-time stability. To guarantee the robustness of the control system under model uncertainties and external disturbances, a disturbance compensation component is incorporated. A Lyapunov-based stability analysis is then carried out to rigorously prove the global finite-time robust stability of the overall system.

1. System description and modeling.

1.1. Experimental setup and operating principle. The study of the motor control algorithm was conducted on an experimental system. Figure 1 illustrates the connection diagram of the motor control model based on a microcontroller platform. The experimental setup for DC motor position control was developed in the Control Systems Laboratory at Le Quy Don Technical University and serves as the research object.

The nominal parameters of the motor were approximately determined through measurements and the manufacturer's datasheet. The YFROBOT Metal Gearmotor GA25 operates at a 12 V DC supply and is equipped with a 34:1 gearbox, which increases torque while reducing rotational speed. Additionally, a Hall-effect encoder is directly mounted on the motor shaft to provide position feedback.

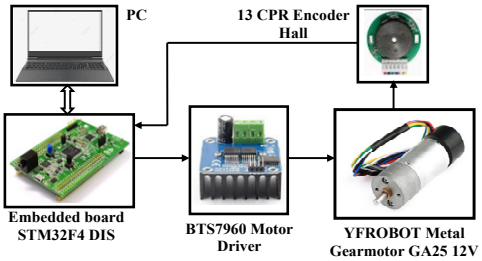

Fig. 1. Block diagram of the experimental DC motor control setup

The embedded controller is implemented on an STM32F411 microcontroller. The microcontroller acquires the motor shaft's angular position through a 13-CPR Hall-effect encoder, whose signals are read via the built-in external interrupt interface. The rotational speed of the motor shaft and the control algorithm are executed within the embedded software. The control signal is generated in the form of PWM using the microcontroller's internal timer and transmitted via GPIO to the BTS7960 motor driver module, enabling the motor to rotate precisely to the desired position.

1.2. Nonlinear mathematical model of the DC motor. The schematic diagram of the DC motor is shown in Fig. 2, where R is the armature resistance, L is the armature inductance, v is the applied voltage, i is the armature current, e is the back electromotive force (back EMF), $J_M = J + \Delta J$ is the load moment of inertia, J is the nominal inertia, ΔJ represents its bounded variation, B is the viscous friction coefficient, τ is the electromagnetic torque generated by the motor, θ is the angular position, and ω the angular velocity of the motor shaft.

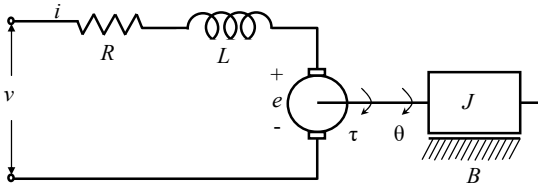

Fig. 2. Model of the permanent magnet DC motor system

The dynamic equations of the DC motor, according to [4], are expressed as

$$\begin{cases} \dfrac{\mathrm{d}\theta(t)}{\mathrm{d}t} = \omega(t); \\ L\dfrac{\mathrm{d}i(t)}{\mathrm{d}t} = v(t) - Ri(t) - k_w\omega(t); \\ J\dfrac{\mathrm{d}\omega(t)}{\mathrm{d}t} = k_i i(t) - B\omega(t) - C\,\mathrm{sgn}(\omega) + d_1(t), \end{cases} \quad (1)$$

where k_w is the back EMF constant; k_i is the motor torque constant, C is the static friction of the motor. The disturbance term $d_1(t)$ accounts for external disturbance torques and model uncertainties (for example, inertia variations ΔJ).

For small-scale DC motors, the control method typically employs PWM signals applied to an H-bridge circuit, which makes accurate and efficient current measurement highly complex. The electrical time constant (L/R) is typically much smaller than the mechanical time constant (J/B). Therefore, the current dynamics reach steady state much faster than the mechanical dynamics. This allows the armature current i to be considered nearly steady, meaning that $i \approx v/R$.

Nevertheless, when operating in high-frequency or large-angle regimes, the inductance L can influence the transient response, and this approximation may require further validation through experimental comparison. Let the state variables be defined as $\theta=x_1$, $\omega=x_2$ and $v=u$. The dynamic model of the DC motor can be rewritten in the following form [5, 8, 10]:

$$\begin{cases} \dot{x}_1 = x_2; \\ \dot{x}_2 = -\dfrac{B}{J}x_2 - \dfrac{C}{J}\operatorname{sgn}(x_2) + \dfrac{k_i}{JR}u + d(t), \end{cases} \quad (2)$$

where $d(t)$ represents both the electrical model uncertainties and the disturbance term $d_1(t)$.

Assumption 1. The disturbance term $d(t)$ is bounded within the interval $(-D, D)$, where D is a positive constant.

In this study, the DC motor is coupled to the load through a gearbox with minimal backlash. The stiffness of the coupling and the gearbox is assumed to be sufficiently high, allowing the elastic effects to be neglected. Therefore, the system can be reasonably modeled as a single-mass electromechanical system rather than a two-mass one. The control objective is to design a finite-time robust position-tracking controller for the DC motor to follow a given reference trajectory $x_{sp}(t)$, based on the incomplete mathematical model (2) in the presence of the disturbance $d(t)$.

2. Synthesis of a finite-time robust position-tracking control law (RFTC) for the DC motor.

2.1. Fundamentals of finite-time control theory.

Consider a nonlinear system that can be described as follows:

$$\dot{\boldsymbol{x}}(t) = f(\boldsymbol{x}(t), \boldsymbol{u}),\ \boldsymbol{x}(0) = \boldsymbol{x}_0\,, \quad (3)$$

where $x \in R_n$ is the state vector of the system; $f(0)=0$. The function $f(\boldsymbol{x})$ is the continuous nonlinear function defined in an open neighborhood around the origin.

Definition 1 [23]. Given an initial time t_0, a positive constant T, and two state sets $\boldsymbol{X}_0$ and $\boldsymbol{X}_t$, system (3) is said to be finite-time stable with respect to (t_0, T, $\boldsymbol{X}_0$, $\boldsymbol{X}_t$) if

$$\boldsymbol{x}_0 \in \boldsymbol{X}_0 \Rightarrow \boldsymbol{x}(t) = \boldsymbol{X}_t, \quad t \in [t_0, t_0 + T], \quad (4)$$

where $\boldsymbol{x}(t)$ denotes the solution of (3) starting from the initial state $\boldsymbol{x}_0$ at time t_0.

Lemma 1 [20]. Assume there exists a continuously differentiable function $V(\boldsymbol{x}) \in C^1$, defined in a neighborhood $U \subset R^n$ of the origin, and real constants $c>0$ and $0<\alpha<1$ such that:

1) $V(\boldsymbol{x})$ is positive definite on U;

2) $\dot{V}(\boldsymbol{x}) + cV^{\alpha}(\boldsymbol{x}) \le 0, \quad \forall \boldsymbol{x} \in U$.

Then, the origin of the system is finite-time stable. The settling time depends on the initial state $\boldsymbol{x}_0$ and satisfies

$$T_x(\boldsymbol{x}_0) \le \frac{V^{1-\alpha}(\boldsymbol{x}_0)}{k(1-\alpha)} \quad (5)$$

for all $\boldsymbol{x}_0$ within some open neighborhood of the origin. If $U=R^n$ and $V(\boldsymbol{x})$ is radially unbounded (i.e., $V(\boldsymbol{x}) \to +\infty$ as $\boldsymbol{x} \to +\infty$), then system (4) is globally finite-time stable at the origin of the coordinate system.

Lemma 2. Consider the strict-feedback system given by

$$\begin{cases} \dot{z}_1 = z_2; \\ \dot{z}_2 = -\lambda \operatorname{sgn}(c_1 z_1 + z_2)\left|c_1 z_1 + z_2\right|^{2\beta-1} + c_1 v_1 \dfrac{z_1}{\sqrt{z_1^2 + \varepsilon^2}} - c_1 z_2, \end{cases} \quad (6)$$

where $v_1>0$, $\varepsilon>0$, $\lambda>0$, $\beta \in (0.5, 1)$, $c_1>0$. Then, system (6) is globally finite-time stable.

Proof. Consider the Lyapunov function

$$V_f = 0.5s^2 = 0.5(c_1 z_1 + z_2)^2\,. \quad (7)$$

Taking the time derivative yields

$$\dot{V}_f = (c_1 z_1 + z_2)(c_1 \dot{z}_1 + \dot{z}_2) =$$

$$= (c_1 z_1 + z_2)\left(-\lambda \operatorname{sgn}(c_1 z_1 + z_2)\left|c_1 z_1 + z_2\right|^{2\beta-1}\right) = -\lambda |s|^{2\beta}.$$

From this, we obtain:

$$\dot{V}_f + 2^{\beta} \lambda V_f{}^{\beta} \le 0\,. \quad (8)$$

From **Lemma 1**, it follows that the virtual system (6) is globally finite-time stable, which guarantees that system (6) evolves on the manifold $s=0$. Next, it is necessary to show that the motion on the manifold $s=0$ drives the system (6) states to the origin $z_1=0$.

With $s=0$, we have

$$z_2 = -c_1 z_1\,. \quad (9)$$

Substituting this into (6) gives

$$\dot{z}_1 = -v_1 \frac{z_1}{\sqrt{z_1^2 + \varepsilon^2}} - c_1 z_1\,. \quad (10)$$

Now, consider estimating the settling time of (10) with the initial condition $z_1(0)=z_{1,0}$ and define t_p as the minimum time after which $|z|$ does not exceed a prescribed value Δ.

To analyze convergence, consider the Lyapunov function

$$V = z_1{}^2\,, \quad (11)$$

whose time derivative is

$$\dot{V} = 2z_1 \dot{z}_1 = -2\left(v_1 \frac{z_1}{\sqrt{z_1^2 + \varepsilon^2}} + c_1\right) z_1{}^2 \le 0\,. \quad (12)$$

From (13), it is evident that the solution of (10) converges to the origin. Moreover, from (12) we obtain

$$\dot{V} \le -2\left(v_1 \frac{z_1}{\sqrt{z_1^2 + \varepsilon^2}} + c_1\right) z_1{}^2; \quad (13)$$

$$\frac{\mathrm{d}V}{V} \le -2\left(v_1 \frac{z_1}{\sqrt{z_1^2 + \varepsilon^2}} + c_1\right) \mathrm{d}t\,. \quad (14)$$

Integrating this inequality for V evolving from V_0, corresponding to the time interval from 0 to t_p, yields

$$t_p \le \frac{\sqrt{z_{1,0}^2 + \varepsilon^2}}{v_1 + c_1 \sqrt{z_{1,0}^2 + \varepsilon^2}} \ln\left(\frac{z_{1,0}}{\Delta}\right). \quad (15)$$

In classical linear control theory, the settling time t_p is defined as the time after which the deviation between the instantaneous response and the steady-state value does not exceed a specified threshold Δ. The results above demonstrate that system (6) is finite-time stable with respect to the manifold $s=0$ and that the state variable z_1

converges to within the prescribed bound Δ in the finite time t_p, determined by the initial conditions and the chosen value of Δ.

Therefore, according to **Definition 1**, it can be concluded that system (6) is globally finite-time stable.

2.2. Synthesis of a robust finite-time control (RFTC) law based on the differential geometric method. To design the finite-time control law u for system (2), it is assumed that the system operates without disturbances, i.e., $d(t)=0$. Based on the differential geometric method, a diffeomorphic transformation is established between the nonlinear system (2) and the virtual system (6) with respect to x_i. Consider the transformation $z_1=x_1-x_{sp}$, where x_{sp} is the desired angular position of the motor shaft. Under this construction, the diffeomorphic transformation is expressed as follows

$$\begin{cases} z_1 = x_1 - x_{sp}; \\ z_2 = x_2 - \dot{x}_{sp} + v_1 \dfrac{z_1}{\sqrt{z_1^2 + \varepsilon^2}}. \end{cases} \tag{16}$$

This means that z_i depends only on x_i. Therefore, by substituting z_2 from the last equation of transformation (16) into the last equation of system (2), and combining it with system (6), the following control law is obtained:

$$u = \frac{JR}{k_i}\begin{pmatrix} \dfrac{B}{J}x_2 + \dfrac{C}{J}\operatorname{sgn}(x_2) + \ddot{x}_{sp} - \varepsilon^2 v_1 \dfrac{x_2 - \dot{x}_{sp}}{\left(z_1^2+\varepsilon^2\right)^{1.5}} \\ -\lambda \operatorname{sgn}(c_1 z_1 + z_2)\left|c_1 z_1 + z_2\right|^{2\beta-1} \\ + c_1 v_1 \dfrac{z_1}{\left(z_1^2+\varepsilon^2\right)^{0.5}} - c_1 z_2 \end{pmatrix}. \tag{17}$$

The control law is acceptable only if a diffeomorphic mapping exists between system (3), when $d(t)=0$, and system (6), meaning that the Jacobian matrix of the mapping between the two systems must be non-singular, which implies that:

$$\det\begin{bmatrix} \dfrac{\partial z_1}{\partial x_1} & \dfrac{\partial z_1}{\partial x_2} \\ \dfrac{\partial z_2}{\partial x_1} & \dfrac{\partial z_2}{\partial x_2} \end{bmatrix} = \begin{vmatrix} 1 & 0 \\ \dfrac{\varepsilon_2 v_1}{\left(z_1^2+\varepsilon^2\right)^{1.5}} & 1 \end{vmatrix} \neq 0. \tag{18}$$

According to **Lemma 2**, the control law (17) guarantees that system (2), in the absence of disturbances, achieves finite-time stability, where the settling time is determined by the sum of the time required for the state to reach the manifold $s=0$ (5) and the time t_p (15).

To mitigate the effect of the disturbance term $d(t)$ on the stability and control performance of the DC motor under control law (17), a disturbance compensation component is further incorporated into the control law as follows:

$$u_r = u - \frac{JR}{k_i}\delta \operatorname{sgn}(c_1 z_1 + z_2). \tag{19}$$

Theorem 1. Under the conditions of parameters $v_1>0$, $\varepsilon>0$, $\lambda>0$, $\beta\in(0.5, 1)$, $c_1>0$, $\delta>\Delta$ and **Assumption 1**, the control law (19) ensures that system (2) is globally asymptotically stable.

Proof. Consider the Lyapunov function defined in (7). Taking its time derivative and substituting from (2), (6), and (9), we obtain:

$$\dot{V}_f = (c_1 z_1 + z_2)\begin{pmatrix} -\lambda \operatorname{sgn}(c_1 z_1 + z_2)\left|c_1 z_1 + z_2\right|^{2\beta-1} \\ -\delta \operatorname{sgn}(c_1 z_1 + z_2) + d(t) \end{pmatrix} = \tag{20}$$

$$= 2^{\beta}\lambda V_f{}^{\beta} - \left|c_1 z_1 + z_2\right|\left(\delta - \operatorname{sgn}(c_1 z_1 + z_2)\mathrm{d}(t)\right).$$

According to **Assumption 1**, if $\delta\geq D$ is chosen, it always follows that $\dot{V}_f \leq 0$. Consequently, system (3) is globally asymptotically stable. The structural block diagram of the DC motor control system employing control law (19) is shown in Fig. 3. It is noteworthy that the saturation blocks in the figure constrain the controller's voltage, considering the electromechanical limits of both the power circuitry and the motor. This ensures that the motor accurately and feasibly tracks the reference trajectory.

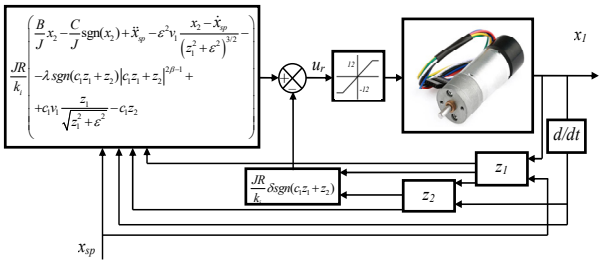

Fig. 3. Block diagram of the DC motor control system

2.3. Design of the SMC law. From system (2), the control signal must be determined so that the control objective $x_1=x_{sp}$ is achieved. The output tracking error of the system is defined as:

$$e_1 = x_1 - x_{sp}. \tag{21}$$

The sliding surface of the controller is chosen as:

$$s = \dot{e}_1 + \gamma e_1. \tag{22}$$

where $\gamma>0$ is the parameter ensuring the asymptotic stability of the sliding surface. Applying SMC theory, we obtain:

$$\left(\dot{x}_2 - \ddot{x}_{sp}\right) + \gamma\left(\dot{x}_1 - \dot{x}_{sp}\right) = -K \operatorname{sgn}(s), \tag{23}$$

where K is the positive constant.

Hence, the SMC law is expressed as:

$$u = \frac{JR}{k_i}\begin{pmatrix} \dfrac{B}{J}x_2 + \dfrac{C}{J}\operatorname{sgn}(x_2) + \ddot{x}_{sp} \\ -\gamma\left(x_2 - \dot{x}_{sp}\right) - K \operatorname{sgn}(s) \end{pmatrix}. \tag{24}$$

3. Simulation and experimental results.

3.1. Simulation results. To validate the effectiveness of the proposed finite-time control law for the DC motor, numerical simulations were carried out in the MATLAB environment. The parameters of the motor and its load in the mathematical model were determined from the datasheet and through direct measurements on the physical system, given as: J = 0.225 kg·m^2; R=9.1 Ω; L=6 mH; C=0.001 N·m; B = 6.25 10^{-5} N·m·s/rad; k_i=6.8 N·m/A, k_w = 0.015 N·m/A. The parameters of the proposed control law, c_1, v_1, λ, β, and ε, were selected to satisfy the global stability conditions derived in the previous section. In this study, these parameters were chosen as: c_1=15, v_1=2, λ=20, β=0.9, ε=0.001 and δ=7. For comparison, the parameters of the SMC were set as K=380, γ=100. To alleviate the chattering phenomenon in the control law (24), the sign function sgn(s) was replaced by a linear saturation function bounded within [–1, 1]. The simulations were performed on the dynamic model of the

DC motor (1) over a period of 10 s, under a disturbance $d_1(t)$ = 5+sin(0.05t), an additional pulse-like external torque was applied to the load, resulting in a total disturbance of $d_1(t)$ +9. The initial conditions of the motor shaft were set to the origin, i.e., x_1=0, x_2=0.

In the first simulation scenario, the reference signal varied over time as follows: from 0 s to 2 s, the desired position was set to x_{sp} = 1 rad; from 2 s to 8 s, x_{sp} = –1 rad; and from 8 s to 10 s, x_{sp} = 0 rad. The simulation results presented in Fig. 4–6 demonstrate that both control laws, SMC and RFTC, enable the DC motor shaft to accurately track the reference signal with negligible steady-state error. As shown in Fig. 4, the position responses during the transient phase reveal that the SMC controller exhibits noticeable oscillations, a longer settling time, and a higher overshoot compared to the RFTC controller (as summarized in Table 1). Figure 5 shows the position tracking errors over time, showing that both controllers quickly eliminate the steady-state error; however, their transient behaviors differ: SMC presents small local oscillations around transition points, while RFTC achieves a smoother response. The most remarkable comparison appears in Fig. 6, where the SMC controller generates high-amplitude control pulses at step transitions, whereas the RFTC provides a smoother and more continuous control signal. During the disturbance period between 3.5 s and 4 s, the angular response, tracking error, and control voltage of the RFTC controller clearly outperform those of SMC. Specifically, the RFTC achieves a faster settling time – approximately 1.25 s shorter – with less oscillation in the control input u and lower overall energy consumption. These findings indicate that when fast response, vibration attenuation, and enhanced robustness and accuracy are required, the RFTC controller proves to be more effective and reliable than the SMC law.

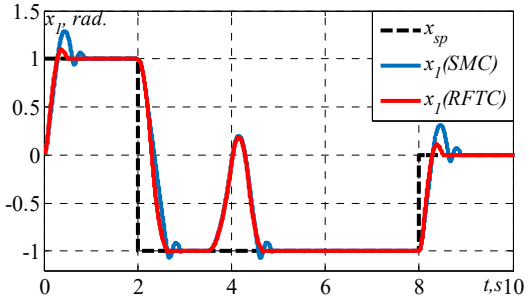

Fig. 4. Position tracking response of the DC motor using RFTC and SMC controllers (1st scenario)

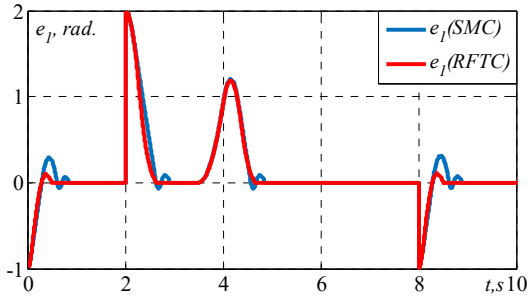

Fig. 5. Position tracking error of the DC motor using RFTC and SMC controllers (1st scenario)

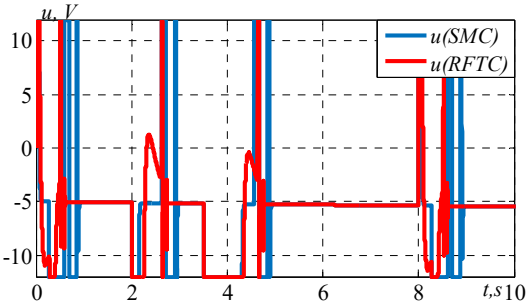

Fig. 6. Control voltage applied to the DC motor using RFTC and SMC controllers (1st scenario)

Table 1

Position response performance indices in the first scenario

Variable	t = (0–2) s		t = (2–8) s		t = (8–10) s	
	RFTC	SMC	RFTC	SMC	RFTC	SMC
Settling time, s	0.5	0.863	0.6	0.94	0.52	0.88
Overshoot, %	10	29.1	0.2	3.6	11	31
Steady-state error, rad	$2.5\cdot10^{-4}$	$4\cdot10^{-4}$	$2.5\cdot10^{-4}$	$4\cdot10^{-4}$	$2.8\cdot10^{-4}$	$4.9\cdot10^{-4}$

In the second simulation scenario, the reference signal was defined as x_{sp}=cos(t)+0.3sin(0.5t). The simulation results presented in Fig. 7–9 demonstrate that both SMC and RFTC control laws achieve effective trajectory tracking performance for the DC motor. As shown in Fig. 7, the position responses obtained using both controllers closely follow the reference trajectory x_{sp}. However, during the transient period, the RFTC controller exhibits a noticeably faster response and avoids the oscillations observed in the SMC controller. In particular, under external disturbances, the RFTC controller provides superior tracking capability and converges more rapidly to the desired trajectory. Figure 8 illustrates the position tracking error, where both controllers achieve very small errors that quickly converge to zero after the initial transient phase. Nevertheless, the proposed RFTC controller yields smaller transient errors. Remarkably, RFTC achieves faster error stabilization with nearly no oscillations, whereas the SMC controller still exhibits local high-frequency oscillations during the early response stage. The control input signals shown in Fig. 9 clearly highlight the distinction between the two methods. The SMC controller generates large-amplitude, abrupt control pulses at the beginning of the response and exhibits chattering under sudden disturbances. In contrast, the RFTC controller produces a smoother and more continuous control signal. This observation suggests that RFTC can effectively reduce vibration and mechanical wear compared to SMC.

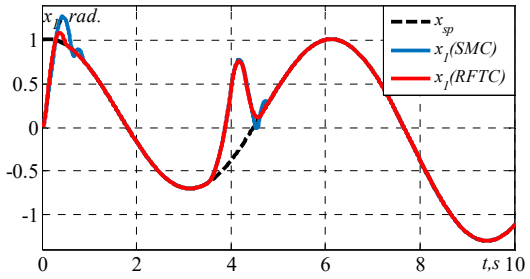

Fig. 7. Position tracking response of the DC motor using RFTC and SMC controllers (2nd scenario)

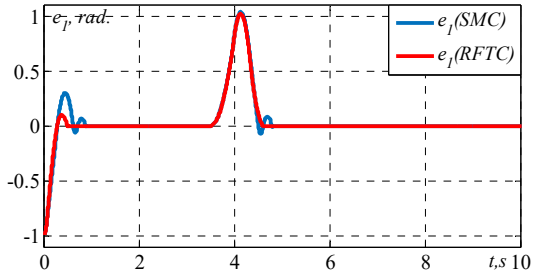

Fig. 8. Position tracking error of the DC motor using RFTC and SMC controllers (2nd scenario)

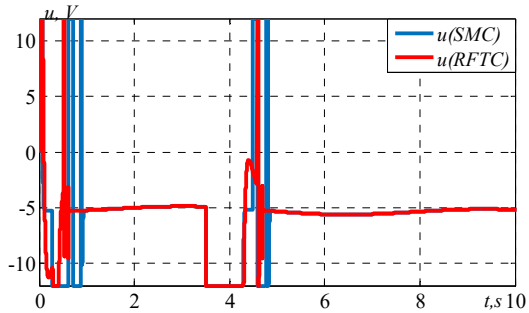

Fig. 9. Control voltage applied to the DC motor using RFTC and SMC controllers (2nd scenario)

3.2. Experimental results. In this section, the objective is to validate the proposed controller on a real-time hardware setup in the laboratory, using the same reference signals as in the previous simulations. The experimental drive system is illustrated in Fig. 10. The motor shaft is coupled with a flywheel-type load to introduce additional inertia. The complete control algorithm was implemented on an embedded STM32 board programmed using STM32CubeIDE, while data acquisition was performed through the STMStudio software.

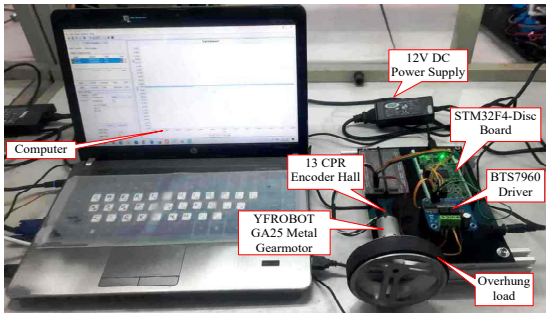

Fig. 10. The experimental drive system

Figures 11, 12 present the angular position responses of the real DC motor system under the SMC and RFTC control laws for two types of reference signals: step and sinusoidal. The results indicate that both controllers ensure satisfactory tracking performance; however, there are noticeable differences in the quality of the responses. For the step reference, both controllers enable the motor shaft to follow the desired trajectory with negligible steady-state error. Nevertheless, the RFTC controller achieves significantly faster response times compared to SMC, with settling times of approximately 0.2 s, 0.5 s, and 0.19 s for each transition, respectively. It should be noted, however, that the proposed controller exhibits a slightly larger overshoot than the SMC controller. When tracking the sinusoidal reference, the RFTC demonstrates superior continuous tracking capability and faster recovery under external disturbances. In contrast, the SMC controller responds more slowly, although it still maintains acceptable tracking accuracy. Furthermore, variations in the SMC controller parameters can lead to oscillations around the reference trajectory. Overall, the experimental results confirm that the RFTC controller provides accurate and well-damped responses in the real system, particularly excelling in fast and smooth tracking of continuous trajectories, while the SMC controller retains its advantage in robustness against disturbances.

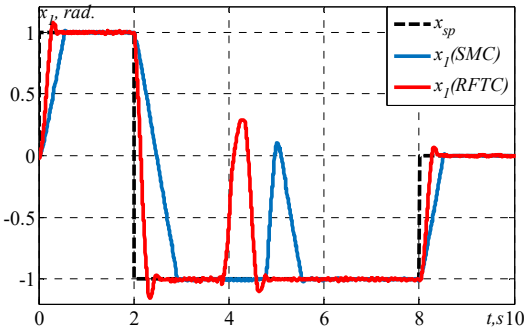

Fig. 11. Position response of the DC motor in the real system under the 1st scenario

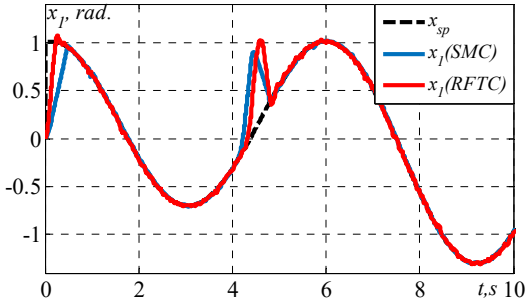

Fig. 12. Position response of the DC motor in the real system under the 2nd scenario

Conclusions. This paper presents a synthesis method for a robust finite-time control law based on differential geometry, applied to position control of a DC motor under external disturbances. The proposed control law guarantees finite-time stability of the system in the presence of model uncertainties and external perturbations. By constructing a virtual system with a nonlinear feedback structure and applying a diffeomorphic transformation, the control law is designed such that the system state trajectories converge to a neighborhood of the equilibrium point within a finite time. The finite-time stability and disturbance rejection capability are rigorously proven using Lyapunov theory. Both simulation and experimental results, compared with the conventional SMC under two reference signal scenarios, demonstrate the superiority of the proposed method. In future work, the authors plan to incorporate observers, neural networks, and fuzzy logic to further improve the performance and overcome the remaining limitations of the proposed control strategy.

Acknowledgements. This work was supported by a university-level research project at Le Quy Don Technical University under Grant No. 25.01.65.

Conflict of interest. The authors declare that they have no conflicts of interest.

REFERENCES

1. Weng C. DC servo motor angle control based on PID control system. *IET Conference Proceedings*, 2024, vol. 2024, no. 19, pp. 1-9. doi: https://doi.org/10.1049/icp.2024.3955.

2. Srinivas G., Durga Sukumar G., Subbarao M. Total harmonic distortion analysis of inverter fed induction motor drive using neuro fuzzy type-1 and neuro fuzzy type-2 controllers. *Electrical Engineering & Electromechanics*, 2024, no. 1, pp. 10-16. doi: https://doi.org/10.20998/2074-272X.2024.1.02.

3. Wang X., Wang S. Adaptive Back-stepping Control of Servo Systems With Asymmetric Dead Zone. *International Journal of Control, Automation and Systems*, 2024, vol. 22, no. 9, pp. 2711-2722. doi: https://doi.org/10.1007/s12555-024-0202-z.

4. Alejandro-Sanjines U., Maisincho-Jivaja A., Asanza V., Lorente-Leyva L.L., Peluffo-Ordóñez D.H. Adaptive PI Controller Based on a Reinforcement Learning Algorithm for Speed Control of a DC Motor. *Biomimetics*, 2023, vol. 8, no. 5, art. no. 434. doi: https://doi.org/10.3390/biomimetics8050434.

5. Garcia-Chica A., Torres-Moreno J.L., Gimenez A. PID Control of DC Actuators. Consideration to Energy Robotic Design. *IFAC-PapersOnLine*, 2024, vol. 58, no. 7, pp. 258-262. doi: https://doi.org/10.1016/j.ifacol.2024.08.071.

6. Dawane M.K., Malwatkar G.M., Deshmukh S.P. Performance improvement of DC servo motor using sliding mode controller. *Journal of Autonomous Intelligence*, 2023, vol. 7, no. 3, art. no. 1162. doi: https://doi.org/10.32629/jai.v7i3.1162.

7. Alnaib I.I., Alsammak A.N., Mohammed K.K. Brushless DC motor drive with optimal fractional-order sliding-mode control based on a genetic algorithm. *Electrical Engineering & Electromechanics*, 2025, no. 2, pp. 19-23. doi: https://doi.org/10.20998/2074-272X.2025.2.03.

8. Du H., Tao L., Deng X., Xu, B. Adaptive Parameter Identification Based Tracking Control of Servo Systems with Unknown Actuator Backlash Compensation. *Actuators*, 2025, vol. 14, no. 6, art. no. 288. doi: https://doi.org/10.3390/act14060288.

9. Wang J., Xu W., Fang S., Chen Y., Wang Y., Wang W. Adaptive control schemes based on characteristic model for servo motor drives. *IET Power Electronics*, 2023, vol. 16, no. 13, pp. 2238-2248. doi: https://doi.org/10.1049/pel2.12544.

10. Song C., Liu J., Yu J., Ma Y., Zhang X., Lv Z. Adaptive Fuzzy Finite-time Tracking Control for A Class of DC Motor with State Constraints. *2020 7th International Conference on Information, Cybernetics, and Computational Social Systems (ICCSS)*, 2020, pp. 682-686. doi: https://doi.org/10.1109/ICCSS52145.2020.9336834.

11. Xu C., Hu J. Adaptive robust control of a class of motor servo system with dead zone based on neural network and extended state observer. *Proceedings of the Institution of Mechanical Engineers, Part I: Journal of Systems and Control Engineering*, 2022, vol. 236, no. 9, pp. 1724-1737. doi: https://doi.org/10.1177/09596518221099783.

12. Sai Lakshmi S., Jeyasenthil R., Babu U.B. Robust controller design based on IMC scheme for motion control of DC servo systems. In: Kumar S., Tripathy M., Jena P. (eds) Control Applications in Modern Power Systems (EPREC 2023). doi: https://doi.org/10.1007/978-981-99-9054-2_16.

13. Yıldırım Ş., Bingol M.S., Savas S. Tuning PID controller parameters of the DC motor with PSO algorithm. *International Review of Applied Sciences and Engineering*, 2024, vol. 15, no. 3, pp. 281-286. doi: https://doi.org/10.1556/1848.2023.00698.

14. Dong Z., Chen S., Sun Z., Tang B., Wang W. A Servo Control Algorithm Based on an Explicit Model Predictive Control and Extended State Observer with a Differential Compensator. *Actuators*, 2025, vol. 14, no. 6, art. no. 281. doi: https://doi.org/10.3390/act14060281.

15. Cui P., Zheng Z., Fu J., Zhang Q., An L. A Fault-Tolerant Control Method for a PMSM Servo Drive System with a Four-Leg Inverter. *Electronics*, 2023, vol. 12, no. 18, art. no. 3857. doi: https://doi.org/10.3390/electronics12183857.

16. Amieur T., Taibi D., Kahla S., Bechouat M., Sedraoui M. Tilt-fractional order proportional integral derivative control for DC motor using particle swarm optimization. *Electrical Engineering & Electromechanics*, 2023, no. 2, pp. 14-19. doi: https://doi.org/10.20998/2074-272X.2023.2.03.

17. Jastrzębski M., Kabziński J., Mosiołek P. Finite-Time, Robust, and Adaptive Motion Control with State Constraints: Controller Derivation and Real Plant Experiments. *Energies*, 2022, vol. 15, no. 3, art. no. 934. doi: https://doi.org/10.3390/en15030934.

18. Nguyen M.H., Ahn K.K. A Finite-Time Disturbance Observer for Tracking Control of Nonlinear Systems Subject to Model Uncertainties and Disturbances. *Mathematics*, 2024, vol. 12, no. 22, art. no. 3512. doi: https://doi.org/10.3390/math12223512.

19. Nguyen X.C., Le D.T. Adaptive finite-time synergetic control for flexible-joint robot manipulator with disturbance inputs. *Electrical Engineering & Electromechanics*, 2025, no. 3, pp. 45-52. doi: https://doi.org/10.20998/2074-272X.2025.3.07.

20. Khatir A., Bouchama Z., Benaggoune S., Zerroug N. Indirect adaptive fuzzy finite time synergetic control for power systems. *Electrical Engineering & Electromechanics*, 2023, no. 1, pp. 57-62. doi: https://doi.org/10.20998/2074-272X.2023.1.08.

21. Chiem N.X., Thuy P.X. A Finite-time Controller Design Based on Strick-feedback System for Flexible Joint Manipulator. *International Journal of Control, Automation and Systems*, 2025, vol. 23, no. 6, pp. 1829-1838. doi: https://doi.org/10.1007/s12555-024-0939-4.

22. Vesović M., Jovanović R., Trišović N. Control of a DC motor using feedback linearization and gray wolf optimization algorithm. *Advances in Mechanical Engineering*, 2022, vol. 14, no. 3. doi: https://doi.org/10.1177/16878132221085324.

23. Ambrosino, R., Ariola, M., Garone, E., Amato, F., & Tartaglione, G. New conditions for finite-time stability of impulsive dynamical systems via piecewise quadratic functions. *IET Control Theory & Applications*, 2022, vol. 16, no. 13, pp. 1341-1351. doi: https://doi.org/10.1049/cth2.12308.

Received 20.08.2025
Accepted 30.10.2025
Published 02.01.2026

Q.B. Nguyen[1], *MSc of Automatic Control,*
X.C. Nguyen[2], *Doctor of Automatic Control,*
[1] Control, Automation in Production and Improvement of Technology Institute (CAPITI), Hanoi, Vietnam,
e-mail: qbinhk37@gmail.com
[2] Department of Automation and Computing Techniques, Le Quy Don Technical University, Hanoi, Vietnam,
e-mail: chiemnx@mta.edu.vn (Corresponding Author)

How to cite this article:
Nguyen Q.B., Nguyen X.C. Finite-time robust position tracking control for DC motors under uncertain dynamics. *Electrical Engineering & Electromechanics*, 2026, no. 1, pp. 44-50. doi: https://doi.org/10.20998/2074-272X.2026.1.06